

## $\beta$ Phase transformations in the Cu–11mass%Al alloy with Ag additions

A. G. Magdalena · A. T. Adorno · T. M. Carvalho ·  
R. A. G. Silva

CBRATEC7 Conference Special Issue  
© Akadémiai Kiadó, Budapest, Hungary 2011

**Abstract** In the Cu–Al system, due to the sluggishness of the  $\beta \leftrightarrow (\alpha + \gamma_1)$  eutectoid reaction, the  $\beta$  phase can be retained metastably. During quenching, metastable  $\beta$  alloys undergo a martensitic transformation to a  $\beta'$  phase at Al low content. The ordering reaction  $\beta \leftrightarrow \beta_1$  precedes the martensitic transformation. The influence of Ag additions on the reactions containing the  $\beta$  phase in the Cu–11mass%Al alloy was studied using differential scanning calorimetry and in situ X-ray diffractometry. The results indicated that, on cooling, two reactions are occurring in the same temperature range, the  $\beta \rightarrow (\alpha + \gamma_1)$  decomposition reaction and the  $\beta \rightarrow \beta_1$  reaction, with different reaction mechanisms (diffusive for the former and ordering for the latter) and, consequently, with different reaction rates. For lower cooling rates, the dominant is the decomposition reaction and for higher cooling rates the ordering reaction prevails. On heating, the  $(\alpha + \gamma_1) \rightarrow \beta$  reverse eutectoid reaction occurs with a resulting  $\beta$  phase saturated with  $\alpha$ . The increase of Ag concentration retards the  $\beta \rightarrow (\alpha + \gamma_1)$  decomposition reaction and the  $\beta \rightarrow \beta_1$  ordering reaction, which occurs in the same temperature range, becomes the predominant process.

**Keywords** Thermal behavior · Eutectoid decomposition · Martensitic transformation · Cu–Al–Ag alloys

A. G. Magdalena (✉) · A. T. Adorno · T. M. Carvalho  
Departamento de Físico-Química, Instituto de Química-Unesp,  
Caixa Postal 355, Araraquara, SP 14801-970, Brazil  
e-mail: aroldogm@iq.unesp.br

R. A. G. Silva  
Departamento de Ciências Exatas e da Terra, Unifesp, Diadema,  
SP 09972-279, Brazil

### Introduction

In the Cu–Al system, the decomposition of the  $\beta$  phase at temperatures below 565 °C involves complex transformations, and a metastable bcc  $\beta_1$  phase is produced by a disorder–order transformation. Subsequently, both  $\beta$  and  $\beta_1$  decompose into the pearlitic  $(\alpha + \gamma_1)$  equilibrium structure. The addition of a third element interferes with the rate of pearlite formation and its final shape [1].

Due to the sluggishness of the  $\beta \rightarrow (\alpha + \gamma_1)$  eutectoid reaction, the  $\beta$  phase can be retained metastably and during quenching metastable  $\beta$  alloys undergo a martensitic transformation [2]. In this study, the thermal behavior of the Cu–11mass%Al alloy with Ag additions was studied using differential scanning calorimetry (DSC) and in situ X-ray diffractometry.

### Experimental

The Cu–11mass%Al, Cu–11mass%Al–4mass%Ag, Cu–11mass%Al–6mass%Ag, Cu–11mass%Al–8mass%Ag, and Cu–11mass%Al–10mass%Ag alloys were prepared in an induction furnace under argon atmosphere, using 99.99% copper, 99.97% aluminum, and 99.98% silver as starting materials. Results from chemical analysis indicated a final composition very close to the nominal one.

Cylindrical samples with 20 mm diameter and 60 mm length were cut in disks with 4.0 mm thickness and small square pieces of about 3.0 mm length were used for DSC analysis. The samples were annealed during 120 h at 1123 K for homogenization. DSC data were obtained using a DSC Q20 TA instruments, with platinum pan and nitrogen flux at about 50 mL min<sup>-1</sup>. The thermal cycles were obtained with a constant heating rate of 20 °C min<sup>-1</sup> and

with rates of cooling equal to 5.0, 1.0, and 0.5 °C min<sup>-1</sup>. In situ X-ray diffraction patterns were obtained at the National Synchrotron Light Laboratory/MCT using the D10BXP X-ray diffraction beam line,  $\lambda = 1.54984 \text{ \AA}$ ,  $E = 7999.80 \text{ keV}$  (Cu–11%Al and Cu–11%Al–4%Ag alloys), and  $\lambda = 0.123984 \text{ \AA}$ ,  $E = 10 \text{ keV}$  (Cu–11%Al–6%Ag, Cu–11%Al–8%Ag, and Cu–11%Al–10%Ag alloys) with solid (not powdered) samples.

## Results and discussion

Figure 1 shows the DSC curves obtained with different heating rates for the Cu–11mass%Al (Fig. 1a) and Cu–11mass%Al–6mass%Ag (Fig. 1b) alloys initially annealed. In Fig. 1a, two endothermic peaks are observed: P<sub>1</sub>, at about 300 °C is associated with  $\alpha_2$  phase disordering and peak P<sub>2</sub>, at about 570 °C, corresponds to the

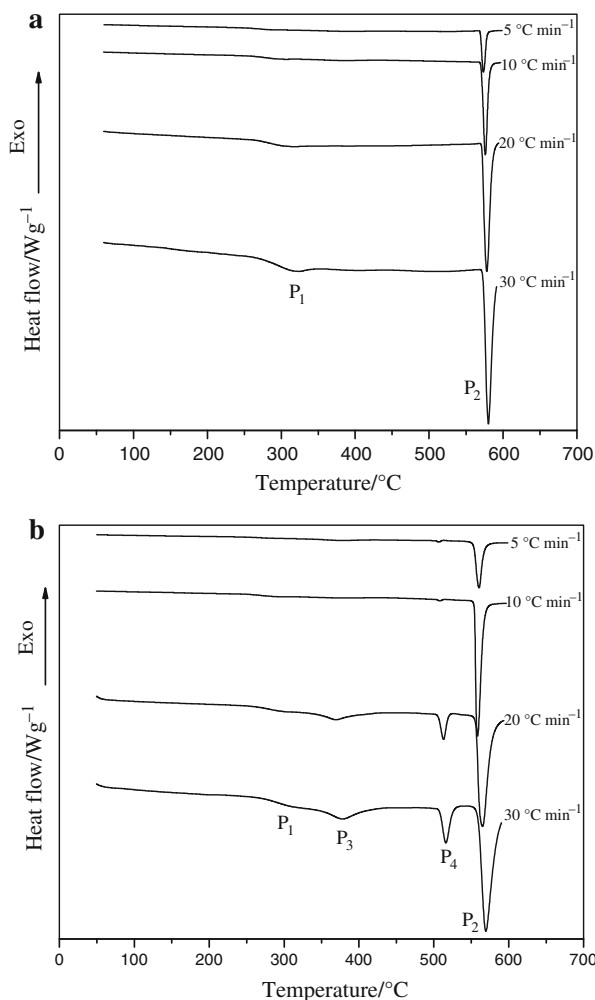


**Fig. 1** DSC curves obtained at different heating rates for alloys initially annealed: **a** Cu–11mass%Al alloy, **b** Cu–11mass%Al–6mass%Ag alloy

( $\alpha + \gamma_1$ )  $\rightarrow \beta$  reverse eutectoid reaction, as expected from the Cu–Al equilibrium diagram [2]. In Fig. 1b, two new thermal events are observed: Peak P<sub>3</sub>, at about 380 °C, is due to the  $\beta' \rightarrow \beta_1$  reverse martensitic reaction and peak P<sub>4</sub>, at about 520 °C, is associated with the  $\beta_1 \rightarrow \beta$  reaction. DSC curves similar to those in Fig. 1a were obtained for the Cu–11mass%Al–4mass%Ag alloy and to those in Fig. 1b for the Cu–11mass%Al–8mass%Ag and Cu–11mass%Al–10mass%Ag alloys. These two new peaks are related with the martensitic phase fraction retained during slow cooling. Depending on the cooling rate, the  $\beta \rightarrow (\alpha + \gamma_1)$  decomposition reaction is not completed, and the retained part of the  $\beta$  phase transforms into the  $\beta_1$  ordered phase prior to the  $\beta_1 \rightarrow \beta'$  reaction which occurs at lower temperatures. On heating, the  $\beta' \rightarrow \beta_1$  reverse martensitic reaction occurs in the same temperature interval of the  $\alpha_2 \rightarrow \alpha$  disordering reaction.

As observed from Fig. 1, the detection of the new thermal events seems to depend on the rates of cooling and heating and on the chemical composition of the alloys. To examine the influence of the heating and cooling rates and of Ag concentration on these transformations, thermal cycles were obtained with a constant heating rate of 20 °C min<sup>-1</sup> and with cooling rates of 5.0, 1.0, and 0.5 °C min<sup>-1</sup> for all studied alloys. Figures 2, 3, and 4 show the thermal cycles obtained, respectively, for the Cu–11mass%Al, Cu–11mass%Al–6mass%Ag, and Cu–11mass%Al–10mass%Ag alloys. In Fig. 2, the exothermic peak observed on cooling, at about 530 °C and the endothermic peak, observed on heating at about 570 °C, correspond, respectively, to the  $\beta \rightarrow (\alpha + \gamma_1)$  and ( $\alpha + \gamma_1$ )  $\rightarrow \beta$  eutectoid reaction. The endothermic peak observed at about 520 °C on heating, in Figs. 3 and 4 and in the enlarged portion of Fig. 2, is associated with the  $\beta_1 \rightarrow \beta$

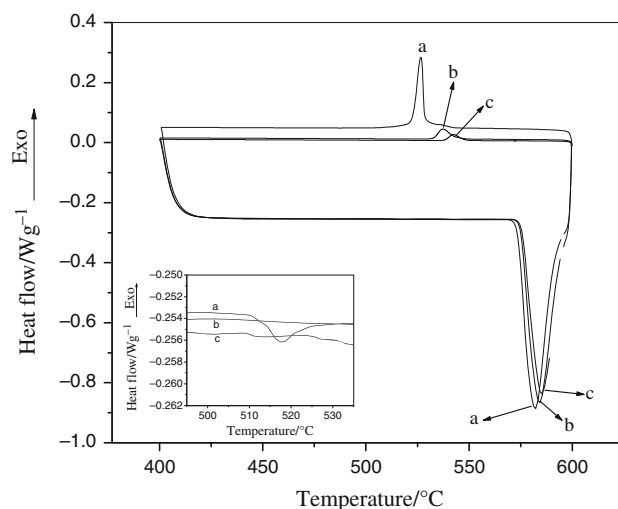


**Fig. 2** Thermal cycles obtained with a constant heating rate of 20 °C min<sup>-1</sup> and with cooling rates of 5.0 (a), 1.0 (b) and 0.5 (c) °C min<sup>-1</sup> for the Cu–11mass%Al alloy initially annealed

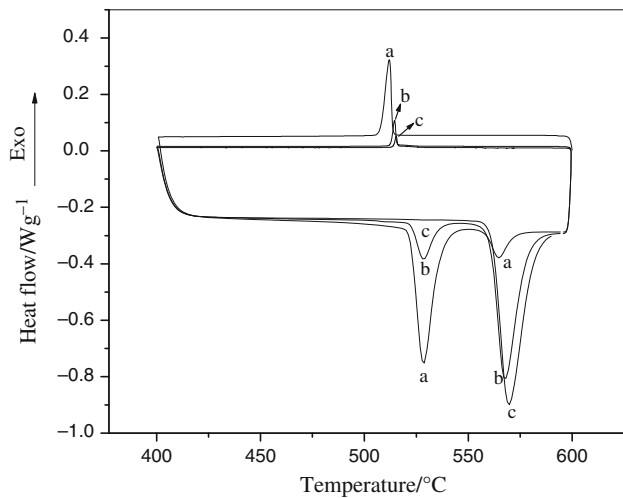


**Fig. 3** Thermal cycles obtained with a constant heating rate of  $20\text{ }^{\circ}\text{C min}^{-1}$  and with cooling rates of  $5.0$  (a),  $1.0$  (b) and  $0.5$  (c)  $^{\circ}\text{C min}^{-1}$  for the Cu–11mass%Al–6mass%Ag alloy initially annealed

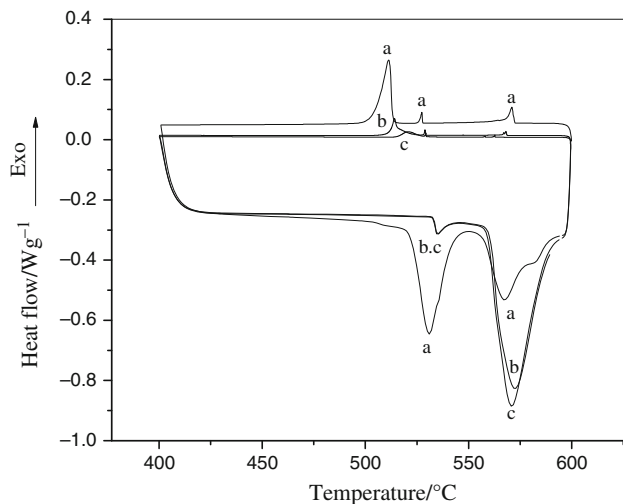


**Fig. 4** Thermal cycles obtained with a constant heating rate of  $20\text{ }^{\circ}\text{C min}^{-1}$  and with cooling rates of  $5.0$  (a),  $1.0$  (b) and  $0.5$  (c)  $^{\circ}\text{C min}^{-1}$  for the Cu–11mass%Al–10mass%Ag alloy initially annealed

reaction. The intensity of this peak is increased with the increase of the cooling rate. As pointed out in the discussion of Fig. 1, the presence of this peak indicates that the  $\beta \rightarrow (\alpha + \gamma_1)$  decomposition reaction was not completed and part of the  $\beta$  phase is retained on cooling. The retained part of the  $\beta$  phase transforms into the  $\beta_1$  ordered phase prior to the  $\beta_1 \rightarrow \beta'$  reaction, which occurs at lower temperatures and on heating, at about  $520\text{ }^{\circ}\text{C}$ , the  $\beta_1 \rightarrow \beta$  reaction occurs. In Fig. 4, two other exothermic peaks were observed on cooling. The first one, at about  $580\text{ }^{\circ}\text{C}$ , corresponds to  $\alpha$  phase precipitation from the saturated  $\beta$  phase and the second one, at

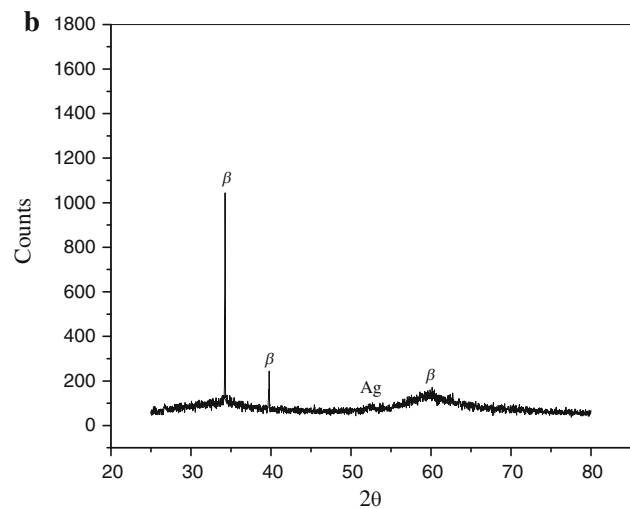
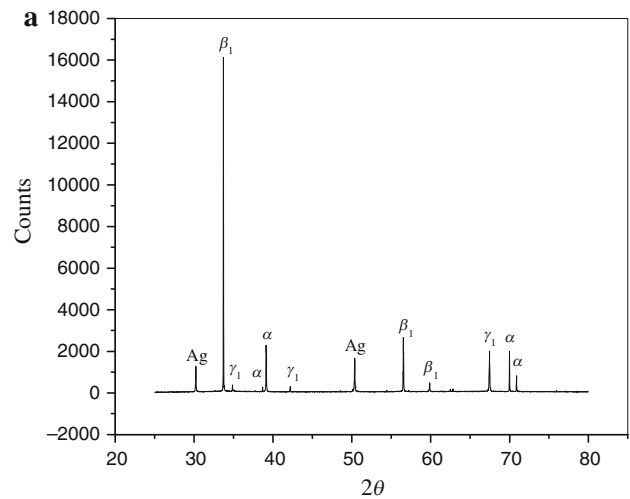


**Fig. 5** In situ X-ray diffraction patterns obtained on heating: **a** for the Cu–11mass%Al–10mass%Ag alloy at about  $480\text{ }^{\circ}\text{C}$  and **b** for the Cu–11mass%Al–8mass%Ag alloy at about  $700\text{ }^{\circ}\text{C}$

about  $530\text{ }^{\circ}\text{C}$ , to Ag precipitation. This  $\alpha$  phase excess is produced on annealing, due to  $\alpha$  phase dissolution in the pearlitic phase, enhanced by the presence of Ag. On heating, the  $(\alpha + \gamma_1) \rightarrow \beta$  reverse eutectoid reaction occurs with a resulting  $\beta$  phase saturated with  $\alpha$ . In this way, the starting condition of the thermal cycles obtained in Figs. 3 and 4 correspond to this saturated  $\beta$  phase. The  $\alpha$  phase excess will disturb the  $\beta \rightarrow (\alpha + \gamma_1)$  decomposition reaction and part of the  $\beta$  phase will be retained on cooling. For the Cu–11mass%Al–10mass%Ag alloy (Fig. 4), the higher Ag content allows the detection of  $\alpha$  and Ag-rich phases precipitation prior to the  $\beta \rightarrow (\alpha + \gamma_1)$  decomposition reaction.

Figure 5 shows the in situ X-ray diffraction patterns obtained for the Cu–11mass%Al–10mass%Ag alloy at about  $480\text{ }^{\circ}\text{C}$  (Fig. 5a) and for the Cu–11mass%Al–8mass%Ag alloy at about  $700\text{ }^{\circ}\text{C}$  (Fig. 5b). In Fig. 5a, it is possible to observe the diffraction peaks corresponding to

the  $\beta_1$ ,  $(\alpha + \gamma_1)$ , and Ag-rich phases and in Fig. 5b those corresponding to the  $\beta$  and Ag-rich phases, thus confirming what were proposed in the discussions of the thermal cycles in Figs. 3 and 4.

It is interesting to observe that the exothermic peak observed at about 530 °C on cooling increases its intensity with the increase of the cooling rate. In this way, when the  $\beta \rightarrow (\alpha + \gamma_1)$  decomposition reaction is not completed and part of the  $\beta$  phase is retained, the observed peak also includes the  $\beta \rightarrow \beta_1$  reaction, which is occurring in the same temperature interval. With the decrease of the cooling rate, the  $\beta$  phase fraction that is not decomposed decreases and the  $\beta$  fraction available for the  $\beta \rightarrow \beta_1$  reaction is also decreased, thus decreasing the peak intensity. Results obtained for Cu–Al alloys near the  $\alpha$ –Cu–Al solubility limit (Al concentration in the range 17–21 at.%) indicated that for cooling rates equal of lower than 1.0 °C min<sup>-1</sup> the endothermic peak corresponding to the  $\beta_1 \rightarrow \beta$  reaction was not observed [3]. The results obtained in this study indicated that for the Cu–11mass%Al alloy the same behavior was observed, but for alloys with Ag additions in the range from 4.0 to 8.0 mass% this endothermic peak is observed for a cooling rate of 1.0 °C min<sup>-1</sup> and not for 0.5 °C min<sup>-1</sup>. Otherwise, for the Cu–11mass%Al–10mass%Ag alloy, the endothermic peak corresponding to the  $\beta_1 \rightarrow \beta$  reaction is observed for all cooling rates considered. On cooling, two reactions are occurring in the same temperature range, the  $\beta \rightarrow (\alpha + \gamma_1)$  decomposition reaction and the  $\beta \rightarrow \beta_1$  reaction, with different reaction mechanisms (diffusive for the former and ordering for the latter) and, consequently, with different reaction rates. For lower cooling rates, the dominant is the decomposition reaction and for higher cooling rates the ordering reaction prevails. Addition of 10 mass%Ag is retarding the decomposition reaction and, for lower cooling rates, the reaction rate is so slow that the dominant process is  $\beta \rightarrow \beta_1$ . This effect is associated with Ag–Al interaction during Al atoms diffusion and the formation of  $\gamma_1$  phase.

The Cu-rich phase of the Cu–Al–Ag alloys is a fcc solid solution of Al and Ag in copper and the high temperature  $\beta$  phase has a bcc structure based on Cu–Al. At elevated temperatures, these phases are both disordered and, on cooling, the  $\beta$  phase order tends to be greater than that of the  $\alpha$  phase, due to the more favorable Cu–Al pairs and to

the presence of Ag. The copper–silver miscibility gap in the Cu–Ag system is the result of the excessive disparity between Cu and Ag atoms (large size factor), while the Ag–Al system is an example of a very small size factor [4]. In this way, Ag solubility is greater in  $\beta$  than in  $\alpha$  phase. At elevated temperatures, Ag–Al interaction in the  $\beta$  phase decreases Al diffusion rate, thus decreasing the  $\beta \rightarrow (\alpha + \gamma_1)$  decomposition reaction rate [5], and the  $\beta \rightarrow \beta_1$  ordering reaction becomes the predominant process.

## Conclusions

The results indicated that, on cooling, two reactions are occurring in the same temperature range, the  $\beta \rightarrow (\alpha + \gamma_1)$  decomposition reaction and the  $\beta \rightarrow \beta_1$  reaction, with different reaction mechanisms (diffusive for the former and ordering for the latter) and, consequently, with different reaction rates. For lower cooling rates, the dominant is the decomposition reaction and for higher cooling rates the ordering reaction prevails. On heating, the  $(\alpha + \gamma_1) \rightarrow \beta$  reverse eutectoid reaction occurs with a resulting  $\beta$  phase saturated with  $\alpha$ . The increase of Ag concentration retards the  $\beta \rightarrow (\alpha + \gamma_1)$  decomposition reaction and the  $\beta \rightarrow \beta_1$  ordering reaction, which occurs in the same temperature range, becomes the predominant process.

**Acknowledgements** The authors thank the support of FAPESP (Project no. 2006/04718-0), CNPq and LNLS-Brazilian Synchrotron Light Laboratory/MCT.

## References

1. Kulkarni SD. Thermodynamics of martensitic and eutectoid transformations in the Cu–Al system. *Acta Metall.* 1973;21: 1461–9.
2. Massalski TB. Binary alloy phase diagrams. 2nd ed. Metals Park: American Society for Metals; 1992.
3. Adorno AT, Guerreiro MR, Benedetti AV. Thermal behavior of Cu–Al alloys near the  $\alpha$ –Cu–Al solubility limit. *J Therm Anal Calorim.* 2001;65:221–9.
4. Adorno AT, Silva RAG. Kinetics of martensite decomposition in the Cu–9Al–6Ag alloy. *J Alloys Compd.* 2005;402:105–8.
5. Magdalena AG, Adorno AT, Silva RAG, Carvalho TM. Effect of Ag concentrations on the thermal behavior of the Cu–10mass%Al and Cu–11mass%Al alloys. *J Therm Anal Calorim.* 2009;97:47–51.